In Vitro Polymerization of Tau Protein Monitored by Laser Light Scattering: Method and Application to the Study of FTDP-17 Mutants †

ARTICLE *in* BIOCHEMISTRY · JUNE 2000

Impact Factor: 3.02 · DOI: 10.1021/bi000201f · Source: PubMed

7 AUTHORS, INCLUDING:

Truman Chris Gamblin
University of Kansas
31 PUBLICATIONS **1,718** CITATIONS
SEE PROFILE

Michael Vitek
Duke University Medical Center
179 PUBLICATIONS **8,919** CITATIONS
SEE PROFILE

Jeff Kuret
The Ohio State University
102 PUBLICATIONS **4,281** CITATIONS
SEE PROFILE

Lester I Binder
Michigan State University
144 PUBLICATIONS **14,074** CITATIONS
SEE PROFILE

In Vitro Polymerization of Tau Protein Monitored by Laser Light Scattering: Method and Application to the Study of FTDP-17 Mutants†

T. Chris Gamblin,*,‡ Michelle E. King,‡ Hana Dawson,§ Michael P. Vitek,§ Jeff Kuret,|| Robert W. Berry,‡ and Lester I. Binder‡

Department of Cell and Molecular Biology and Cognitive Neurology and Alzheimer's Disease Center, Northwestern University Medical School, 303 E. Chicago Avenue, Chicago, Illinois 60611-3008, OSV, Inc., and Division of Neurology, Duke Medical Center, Durham, North Carolina 27710, and Department of Medical Biochemistry, Ohio State University Medical School, Columbus, Ohio 43210

Received February 1, 2000; Revised Manuscript Received March 20, 2000

ABSTRACT: Tau polymerization into the filaments that compose neurofibrillary tangles is seminal to the development of many neurodegenerative diseases. It is therefore important to understand the mechanisms involved in this process. However, a consensus method for monitoring tau polymerization in vitro has been lacking. Here we demonstrate that illuminating tau polymerization reactions with laser light and measuring the increased scattering at 90° to the incident beam with a digital camera results in data that closely approximate the mass of tau polymer formation in vitro. The validity of the technique was demonstrated over a range of tau concentrations and through multiple angle scattering measurements. In addition, laser light scattering data closely correlated with quantitative electron microscopy measurements of the mass of tau filaments. Laser light scattering was then used to measure the efficiency with which the mutant tau proteins found in frontotemporal dementia and Parkinsonism linked to chromosome 17 (FTDP-17) form filamentous structures. Several of these mutant proteins display enhanced polymerization in the presence of arachidonic acid, suggesting a direct role for these mutations in tau the filament formation that characterizes FTDP-17.

The microtubule-associated protein tau is a soluble protein that is normally involved in the maintenance of the neuronal cytoskeleton (*1*). Many neurodegenerative diseases, however, are characterized by the abnormal aggregation of this tau molecule into largely insoluble filamentous structures (reviewed in ref *2*). For example, the degree of dementia in Alzheimer's disease (AD),[1] the most common dementing illness, is significantly correlated with the appearance and distribution of neurofibrillary tangles, whose structures are mainly composed of tau filaments (*3, 4*), suggesting that tau polymerization is a crucial event in AD. In addition, an abundance of genetic evidence has accumulated recently indicating that altered tau expression or structure causes neurodegenerative diseases (*5*−*12*). Although these diseases differ in the morphological types of filamentous structures which are formed and in the cellular and regional distribution of these structures in the brain, they have been loosely classified as *f*ronto*t*emporal *d*ementia and *P*arkinsonism linked to chromosome *17* (FTDP-17) (*13*); all exhibit tau pathology in the absence of other classical pathological structures, such as β-amyloid deposits (reviewed in ref *2*).

The prominence of tangles in these diseases underscores the need to understand the different mechanisms which might lead to tau polymerization. The simplest approach to this goal has been to study tau polymerization in vitro. "Inducer molecules" have been identified which, when added to solutions of monomeric tau or dimerized tau, result in the formation of filamentous structures. The compounds that have been used to induce tau polymerization include polyanionic macromolecules such as heparin (*14*−*19*), RNA (*20*), and polyglutamate (*15*). In addition, our laboratory has shown that the addition of polyunsaturated free fatty acids such as arachidonic acid (AA) is capable of stimulating physiological concentrations of monomeric tau protein to form filaments similar in morphology to those found in AD (*21*). These synthetic filaments also resemble authentic AD filaments by their immunoreactivity with antibodies designed to detect protein conformations associated with paired-helical filaments and by their ability to bind thioflavin-S (*22*). In addition, authentic paired-helical filaments (PHF) isolated from human brain tissue can be used to seed the growth of synthetic tau (*22*).

One impediment to studying tau polymerization in vitro has been the lack of a consensus method for measuring this process. Among the different techniques which have been employed are sedimentation assays (*16, 23*), qualitative

† Supported by grants from the NIH (AG14453, AG14452, AG15307, AG15383) and the Alzheimer's Association (Zen-98-012, PRG-1709).

* To whom correspondence should be addressed. Tel: (312) 503-0824. Fax: (312) 503−7912. E-mail: t-gamblin@nwu.edu.

‡ Northwestern University Medical School.

§ Duke Medical Center.

|| Ohio State University Medical School.

[1] Abbreviations: AD, Alzheimer's disease; FTDP-17, *f*ronto*t*emporal *d*ementia and *P*arkinsonism linked to chromosome *17*; AA, arachidonic acid; SF, straight filament; PHF, paired-helical filament; ThS, thioflavin-S; EM, electron microscopy; LLS, laser light scattering; HEPES, *N*-2-hydroxyethylpiperazine-*N*′-2-ethanesulfonic acid; DTT, dithiothreitol; i_s, intensity of scattered light.

10.1021/bi000201f CCC: $19.00
Published on Web 04/29/2000

electron microscopy (*14*, *18*, *24*, *25*), quantitative electron microscopy (*21*, *22*, *25*−*28*), and the use of dyes which fluoresce upon binding to aggregates of tau (*15*, *22*). A standard method to assess the polymerization of other filamentous macromolecular compounds is the measurement of the turbidity of protein solutions following the induction of polymerization (*29*). However, turbidimetric analysis requires that enough filaments be formed to cause a decrease in the amount of light transmitted through a protein solution, and this technique has not proven sensitive enough to measure tau polymerization at physiological protein concentrations (1−4 μM). Earlier experimentation has shown 90° light scattering to be a more sensitive method than conventional turbidity measurements, and this method has been used successfully to monitor the assembly of an ancestral homologue of tubulin, FtsZ (*30*). This, in addition to the long history of the use of light scattering for following the assembly of macromolecules in solution, led us to investigate its utility in monitoring tau polymerization in vitro.

Employing laser illumination of the sample to increase sensitivity, we demonstrate that light scattering is a useful indirect method for measuring tau polymerization in vitro, in that under our conditions the intensity of scattering is proportional to the mass of polymerized tau filaments. Laser light scattering (LLS) has been employed to estimate the critical concentration of AA-induced assembly and to study the effects of disease-causing point mutations on tau polymerization. Furthermore, using this method we have found that several mutant forms of tau that are associated with FTDP-17 appear to enhance the fatty-acid induction of tau polymerization in vitro.

EXPERIMENTAL PROCEDURES

Tau Proteins. Full length recombinant human tau protein (HT40) was obtained from a His-tagged construct as described previously (*31*). Site-directed mutagenesis was used to introduce missense mutations (G272V, P301L, V337M, and R406W) into a human tau cDNA clone encoding a 441 amino acid tau protein with four microtubule binding domains in a pGL3 vector. Mutagenesis was performed with a Promega Gene Editor kit according to the manufacturers instructions. The following oligonucleotides were used to create the different mutations as follows: 5′-CAGCCGGGAGTCGGGAAGGTG-3′ for G272V, 5′-AACACGTCCTGGGAGGCGG-3′ for P301L, 5′-GGTGGCCAGATGGAAGTAAATC-3′ for V337M, and 5′-ACGTCTCCATGGCATCTCAG-3′ for R406W. Mutated DNAs were then subcloned into the pT7c-htau23 expression vector using native BstBI/NheI restriction sites to create four tau cDNA (exons 1−5, 7, 9−14) constructs, each with a unique mutation. The identity and position of each mutation in these mutated tau cDNAs was confirmed by automated DNA sequencing using a Perkin-Elmer/Applied Biosystems Dye Terminator Cycle Sequencing Read Reaction DNA Kit, an ABI 373A DNA sequencer, and MacVector DNA sequence analysis software. The protein was then purified in the same manner as wild-type HT40 (*31*).

Arachidonic Acid. Arachidonic acid (AA) was purchased as a 100 mg/mL stock in ethanol from Cayman Chemicals and stored at −20 °C. Working solutions were made by dilution to 2 mM with 100% ethanol immediately before use in single experiments and then discarded.

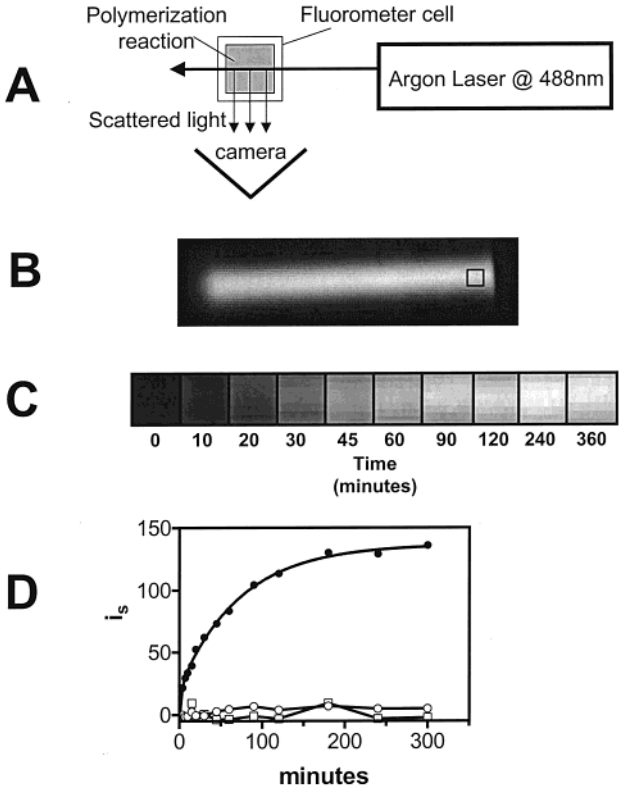

FIGURE 1: Diagram of the method. (A) Schematic representation of a top view (along the axis of polarization) of the LLS apparatus. (B) A digitally captured image of light scattering resulting from a mixture of 4 μM full length human tau protein (HT40) and 75 μM arachidonic acid (AA) after 180 min of polymerization. The box corresponds to the region of the image used to determine the average value of intensity of the scattered light (i_s). (C) An example of the increase in intensity of LLS over time during a tau polymerization reaction. (D) A plot of i_s versus time for a typical polymerization reaction at 4 μM HT40 and 75 μM AA (●). The curve through the data was drawn by using a single-phase exponential association equation. Control reactions of 75 μM AA without the addition of tau protein (○) and 4 μM tau in the absence of AA (□) are also included on the graph.

Polymerization Reactions. Tau polymerization was induced by thoroughly mixing HT40 in the presence of 75 μM arachidonic acid in buffer containing 10 mM HEPES, pH 7.6, 100 mM NaCl, and 5 mM dithiothreitol (DTT) at room temperature and then incubating without stirring. The final concentration of the ethanol vehicle in the polymerization reaction was 3.75%, and this concentration of ethanol was added to control solutions in the absence of AA.

Right Angle Laser Light Scattering. A Lexel model 65 ion laser at a 5 mW setting, tuned to 488 nm, was used to illuminate polymerization reactions with vertically polarized light in 5 mm path length (1.7 mL capacity) fluorometer cells (PGC Scientific). An Electrim Corp. model EDC1000HR digital camera with a 25 mm lens was placed at an angle of 90° to the incident light and perpendicular to the direction of polarization (Figure 1A). The use of a camera to capture the scattered light eliminates the necessity for using slits to block extraneous scattering from angles other than 90°. Images from the camera were collected using HiCam ′95 (Figure 1B). This software was written by Dr. Guenter Albrecht-Buehler, Northwestern University Medical School,

specifically to control the camera and can be downloaded from the website http://www.basic.nwu.edu/g-buehler/hi-cam.htm. Most images were collected using an exposure time of 200 ms with an aperture setting of F8. These settings were adjusted on occasion to compensate for variations in signal intensity. Individual exposures were imported into Adobe Photoshop 5.0 where the marquee tool was used to select a region of interest (10 × 10 pixels) within the scattered light near the front edge of the cuvette, to reduce the amount of signal loss due to prior scattering (Figure 1B). The average gray value of the pixels in the region of interest (intensity of scattered light, or i_s) was obtained using the histogram feature (Figure 1C shows examples of regions of raw data obtained during a polymerization reaction). The gray values range from 0 (black) to 255 (white). Values greater than 255 are possible by reducing the exposure time of the camera, determining the gray value of the scattered light (on a scale of 0−255), and then mathematically compensating for the difference in exposure time. The amount of background scattering was subtracted by measuring the scattering of polymerization reactions without the inducer present or by measuring the scattering of polymerization reactions with inducer present but prior to the addition of tau. The values of background-corrected light scattering were then plotted against time to obtain the time courses for polymerization (Figure 1D). For simple comparisons between experiments, lines were drawn through the polymerization curves using a single-phase exponential function with GraphPad Prism (GraphPad Software):

$$Y = Y_{max}(1 - e^{-KX}) \quad (1)$$

Here the value of Y ascends from zero to Y_{max} with a rate constant K. The use of this equation is not meant to imply any particular model of polymerization.

Electron Microscopy. Samples were removed from the polymerization reaction, fixed in 2% glutaraldehyde, and prepared for electron microscopy by floating a carbon-coated Formvar grid on 10 μL of sample for 1 min followed by staining with 2% uranyl acetate for 1 min. A JEOL 1220 transmission electron microscope operating at 60 kV was used to view the grids. Images were captured at 20 000× using a MegaPlus model 1.6I AMT digital Kodak camera controlled by the AMT camera controller software package. All images were processed and analyzed as described previously (*22, 28*).

RESULTS

Tau Polymerization Induces an Increase in 90° Laser Light Scattering. The amount of right angle laser light scattering (LLS) from tau polymerization reactions in the presence of arachidonic acid (AA) can be measured at rapid intervals and in real time, providing a detailed analysis of the assembly process (see Experimental Procedures and Figure 1). The resulting polymerization curve measured by the increase in LLS (intensity of scattered light, or i_s) attained apparent equilibrium within 7 h and appeared similar in form to other macromolecular assembly reactions monitored by different light scattering techniques (*29*). Nonetheless, the degree to which the intensity of scattered light in this technique reflects the total polymerized mass of tau is critical to the interpretation of these experiments and to the future use of this method

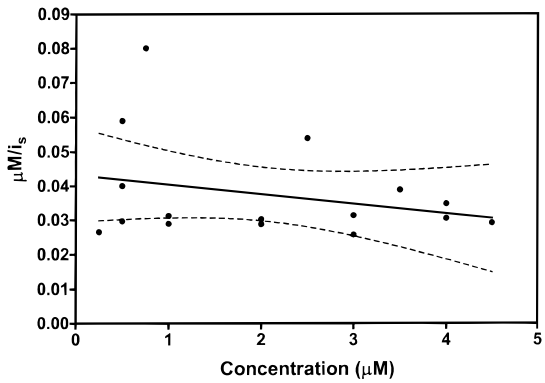

FIGURE 2: Analysis of the relationship of concentration of tau to the intensity of scattering over a range of tau concentrations. Polymerization reactions were performed at tau concentrations from 0.25 to 4.5 μM (*x*-axis). The total concentration of protein used in the polymerization reaction was divided by the maximum values for the intensity of scattered light obtained (*y*-axis). The data were fit to a straight line by linear regression (solid line), and the 95% confidence intervals are shown as dashed lines. The slope of the line was −0.0028 ± 0.0026 (essentially zero).

to study other aspects of tau polymerization. Accordingly, additional tests of the validity of this method were performed.

Validation of the Method. Theoretically, the scattering of polarized light by particles whose dimensions are comparable to the wavelength of the incident beam reduces to the fundamental equation (*32*)

$$\frac{KC}{i_s} = \left(\frac{1}{P(\Theta)}\right)\left(\frac{1}{M_w} + 2BC\right) \quad (2)$$

where K is a constant which takes into account the geometry of the apparatus, the wavelength and intensity of the incident beam, and the indices of refraction of the solute and the solvent. C is the weight concentration of polymer, B is the second virial coefficient, and M_w is the weight-averaged molecular weight of the scattering particles. $P(\Theta)$, which is of particular interest in the present context, is a factor which expresses the angular dependence of scattering when the particle's dimensions are not negligible with respect to the wavelength of light. It is important to determine whether this parameter remains constant under the conditions of our assay, for only then will changes in i_s linearly reflect changes in the mass of scattering material.

By the above equation, when P(Θ) is constant, a plot of C/i_s versus C over a range of tau concentrations should yield a straight line with a slope proportional to B and a *y*-intercept that is inversely proportional to $M_wP(\Theta)$. To generate a plot of this type, tau polymerization reactions were performed over a wide range of concentrations (0.25−4.5 μM) and monitored by right angle LLS. The measurement of i_s was taken at the plateau for each concentration and plotted as in Figure 2. When the data were fit to a linear regression, the slope of the fit was not significantly different from zero, implying that the second virial coefficient (B) is negligible. More importantly, the value of C/i_s does not change significantly with increasing concentrations of tau, implying that $P(\Theta)$ is not greatly influenced by increasing filament length. However, it should be noted that at low tau concentrations (<1 μM) the LLS measurements appear to be less reliable.

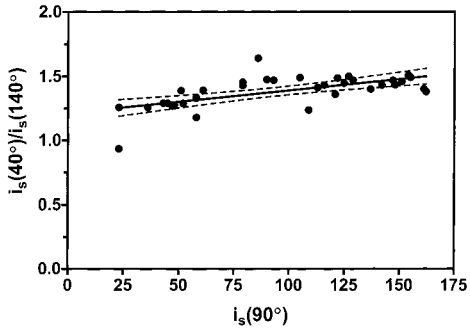

FIGURE 3: Analysis of the angular dependence of tau polymerization reactions. Several different polymerization reactions were performed at low tau concentrations (0.5−2.0 μM). At various times during the polymerization reactions, the camera was moved with respect to the incident light to capture digital images at three different angles (corrected for the refractive indices of glass and water): 40°; 90°; 140°. The ratio of light scattered at 40 and 140° (*y*-axis) was plotted as a function of the intensity of the scattered light at 90° (*x*-axis). The data were fit to a straight line by linear regression (solid line), and the 95% confidence intervals are shown as dotted lines. The slope of the fitted line was 0.0018 ± 0.0004.

Angular Dependence of LLS. A second means of assessing the influence of polymer dimensions on light scattering derives from the fact that $P(\Theta)$ is a function not only of the dimensions of the scattering particle but also of Θ, the angle between the incident beam and the detector. The angular dependence of scattering thus provides a measure of $P(\Theta)$. Under conditions where $P(\Theta)$ is constant with respect to the size of the scattering unit, its angular dependence should not change with the concentration of scattering units. To test this, measurements of scattering at 60 and 120° (40 and 140° after making corrections for the refractive indices of glass and water) with respect to the incident beam were made at initial tau concentrations ranging from 0.5 to 2.0 μM. The ratio of i_s at these angles did not vary to a large degree at 90° scattering values above ca. 25 (Figure 3). Although the linear regression of the data did have a significantly positive slope, its value was very small (0.0018). This implies that changes in i_s within this range of concentrations are largely independent of changes in polymer length, remaining directly proportional to polymer mass. This is not surprising since the average length of the filaments formed is not long with respect to the wavelength of the incident beam of light (Figure 4). Even in the filament population that contains the longest filaments formed (Figure 4D), the average filament length was only 81 nm. In addition, 65% of the total filament population had a theoretical radius of gyration less than $^1/_{20}$ of a wavelength of light ($R_G = L/\sqrt{12}$) (*32*). Filaments below this limit should have $P(\Theta)$ values approaching unity and thus have no measurable angular dependence. However, for a heterogeneous distribution of filament lengths, this analysis may be more complicated (see Discussion).

Linear Relationship of LLS to Tau Concentration. According to eq 2, when $P(\Theta)$ is constant and the second virial coefficient (B) is negligible, the intensity of scattered light should increase linearly with increased polymer mass. To confirm whether this is true for our conditions, the data in Figure 2 were replotted as the intensity of scattered light versus the concentration of tau protein. As expected, i_s increased linearly with the tau monomer concentration (Figure 5) where the best fit of the line had a r^2 value of 0.93 and an *x*-axis intercept at 0.11 μM. The *x*-axis intercept

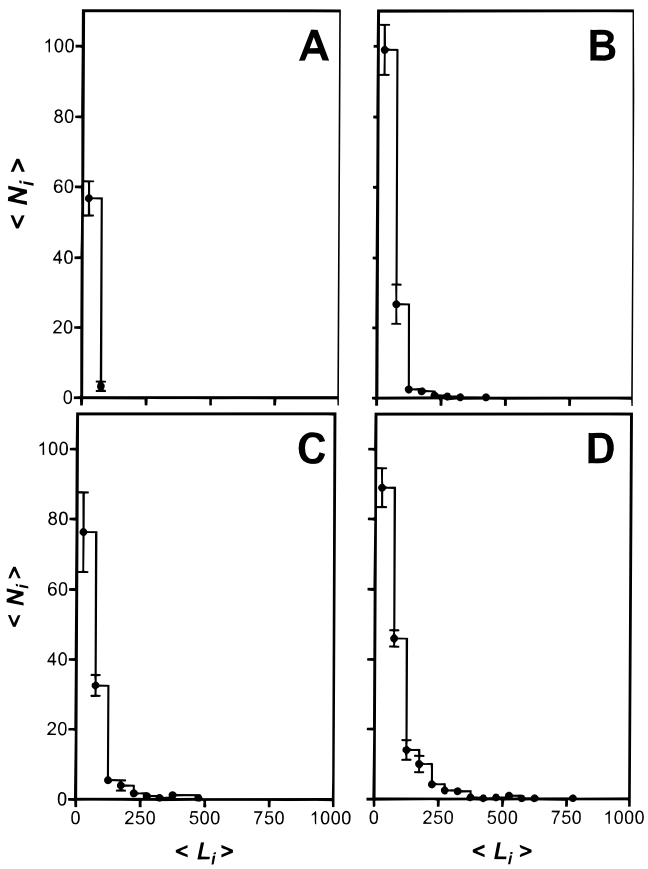

FIGURE 4: Distribution of tau filament lengths at apparent steady state. Polymerization reactions consisting of (A) 0.75 μM, (B) 2.5 μM, (C) 3.5 μM, and (D) 4.5 μM tau plus 75 μM AA were monitored by LLS until an apparent steady state was reached (6 h). A region from each of four electron micrographs for each concentration was used to manually measure the lengths of individual filaments. The length distributions were generated using a 50 nm bin width with the first bin centered at 25 nm. The average number of filaments ($< N_i >$, *y*-axis) at each length ($< L_i >$, *x*-axis) is shown by solid circles (± one standard deviation) connected by a solid line. The scale is the same for all four panels.

is the lower limit of tau protein which would be required for the induction of polymerization by 75 μM AA and therefore represents an estimate of the critical concentration for polymerization. This value is similar to a previous estimate of the critical concentration of tau polymerization (0.50 μM) as measured by thioflavin-S binding (*22*).

Comparison of Quantitation by LLS and Electron Microscopy. As a final test of the validity of LLS, the estimates of the extent of tau polymerization at various tau concentrations obtained by this method were compared to polymer mass measurements resulting from our quantitative electron microscopy assay described previously (*22*, *28*). A direct comparison of this type does not require mathematical treatments of LLS data and provides an independent assessment of the validity of the LLS technique. Four different tau concentrations were used in polymerization reactions and monitored by right angle LLS. When the polymerization reactions reached apparent equilibrium (after 6 h of polymerization), samples were removed and processed for quantitation by electron microscopy (Figure 6A−D). The amounts of LLS (i_s) and total polymer mass (μm/field) were plotted together on separate scales (Figure 6E). The relative amounts of polymer mass measured were similar for each

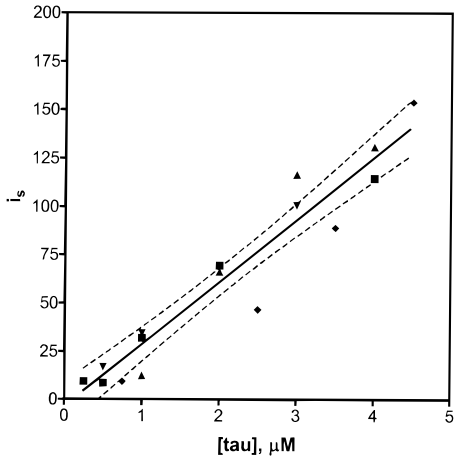

FIGURE 5: Concentration dependence of steady-state luminosity. Polymerization reactions consisting of 75 μM AA and various concentrations of HT40 were performed and monitored as previously described. The maximum scattering values (i_s) from experiments performed on four separate days (represented by the different symbols ■, ▲, ▼, and ◆) were plotted against the concentration of HT40 (μM). The points were fit to a straight line by linear regression (dashed lines represent the 95% confidence interval of the fit). The fit of the line had an r^2 value of 0.93 and extrapolation to the *x*-axis yielded a value of 0.11 μM. Four of the points (represented by ◆) were further analyzed by quantitative electron microscopy in Figure 6.

method, again indicating that LLS is a valid technique for approximating the total mass of tau polymer in vitro.

Application of LLS To Study the Effects of FTDP-17 Mutations. We applied the LLS procedure to examine the assembly properties of missense mutations in the tau gene that cause single amino acid substitutions in tau protein; these mutations are known to cause FTDP-17 (*33*). Tau protein containing a proline to leucine mutation at position 301 (P301L) had the most dramatic effect, in that both the apparent rate and extent of polymerization were significantly increased over that of wild-type tau protein (Figure 7). The tau construct with an arginine to tryptophan mutation at amino acid 406 (R406W) resulted in polymer formation with an equilibrium scattering value as great as P301L but with this value being achieved at a slower apparent rate (Figure 7). The valine to methionine mutation at position 337 (V337M) polymerized better than wild type with regard to equilibrium scattering values but not as well as the P301L mutant. Although the extent of polymerization of the V337M mutant was less than that of the R406W mutant, the two exhibited similar rates of polymerization. By contrast, the glycine to valine mutation at position 272 (G272V) had little apparent effect on tau polymerization, in that the equilibrium amount of polymer formed was similar to wild-type protein. However, the G272V mutant did display a modestly accelerated rate of polymerization when compared to wild-type HT40. These data (summarized in Table 1) show that missense mutations within the tau protein can alter the rate and extent of arachidonic acid-induced polymerization in vitro.

DISCUSSION

Importance of Tau Polymerization. The appearance of filamentous tau deposits is a common event in many neurodegenerative diseases (*2*). However, the role that tau-

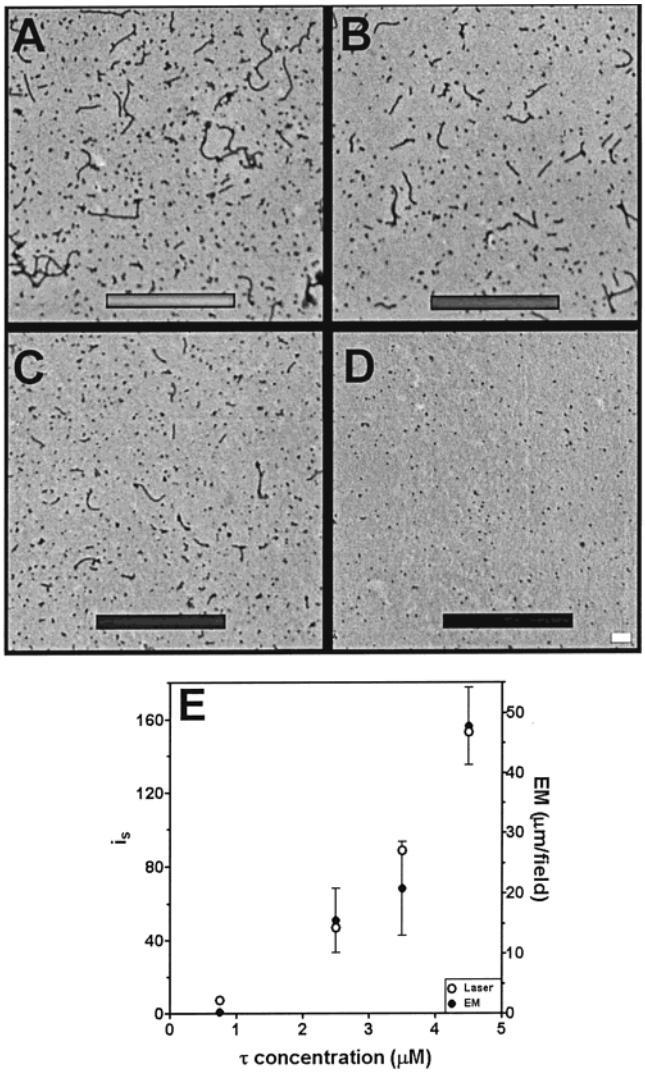

FIGURE 6: Correlation of LLS and electron microscopy. Polymerization reactions using four different concentrations of HT40 were monitored by LLS for 6 h at room temperature. Representative digital electron micrographs taken at a magnification of 20 000× are shown for (A) 4.5 μM, (B) 3.5 μM, (C) 2.5 μM, and (D) 0.75 μM. The digital images of LLS are shown as insets for each of the concentrations. The size bar (white) found in panel D represents 200 nm and is applicable to each panel. (E) Values for LLS (○) and electron microscopy quantification (●) at four different tau concentrations are shown together on different scales, i_s (left axis) and μm/field (right axis), respectively.

containing pathological structures play in the etiology of neurodegeneration is still a matter of active debate. Alzheimer's disease (AD), the most common of these diseases, contains two different major pathological structures: senile plaques consisting mainly of amyloid β protein (Aβ) fibrils and neurofibrillary tangles consisting mainly of tau filaments. It remains unclear how these different abnormal proteinaceous deposits are related to each other and to the dysfunction of neurons in AD. However, recent discoveries of mutations in the tau gene that cause FTDP-17 demonstrate that tau is directly involved in the neurodegenerative process (*33*). Even in FTDP-17 diseases where tau is most certainly involved, it is not known whether the critical event leading to neurodegeneration is a loss of function (i.e. microtubule destabilization) or a toxic gain of function (i.e. blocking intracellular transport in neurons and/or glia) when normally soluble tau enters into a filamentous state. One key piece of

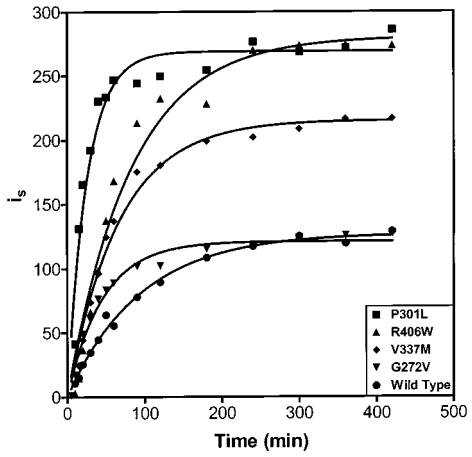

FIGURE 7: Differential effects of FTDP-17 mutations on tau polymerization. Polymerization reactions were performed at 4 μM total protein and monitored by right angle LLS. The values of the intensity of scattered light (i_s, *y*-axis) are shown as a function of time (minutes, *x*-axis) for wild-type HT40 (●), G272V (▼), V337M (◆), R406W (▲), and P301L (■). As a convenience for comparison, lines were drawn through the data using a single-phase exponential association equation (see Experimental Procedures).

evidence that suggests a toxic gain of function for polymeric tau is the cellular degeneration that is observed when human tau protein forms filamentous deposits following overexpression in lamprey central neurons in situ (*34*). This evidence indicates that the polymerization of tau protein directly causes neurodegenerative diseases such as FTDP-17 and is a probable causative event in the development of AD. Proof of a toxic gain of function, however, requires further efforts including sufficient expression of human tau proteins in a mammalian neuron that may induce filament formation, neurofibrillary tangle development, and/or neuronal dysfunction and death.

Although at least three different morphologies of tau filaments have been described in different dementias—paired-helical filaments (PHFs), straight filaments (SFs), and twisted ribbons—it is very likely that the cause of dementia is not the morphological structure of the filaments but rather the presence of *any* tau filaments (*2*). Moreover, the type of dementia that results from pathological tau polymerization is most likely determined by the brain region in which the filament formation and deposition occurs. Thus, tau polymerization can be viewed as the single molecular event linking a broad range of dementing diseases.

In view of the proposed central role of this process in the etiology of neurodegenerative diseases, it is important to gain a better understanding of the different mechanisms that can lead to tau self-association, as such knowledge could lead to the development of therapeutic strategies based on inhibiting this process. Our laboratory has focused on dissecting the molecular mechanisms of this process using the in vitro paradigm of arachidonic acid induction of tau self-association (*21*). The synthetic filaments which are formed in this paradigm are virtually identical to authentic filaments both immunologically and morphologically, suggesting that the arachidonic acid induction of tau polymerization is an acceptable paradigm for studying tau polymerization (*22*).

Techniques for Monitoring Tau Polymerization. To facilitate these studies, we have sought an improved method for measuring tau polymerization. The two major techniques that have been used previously for the investigation of tau polymerization are thioflavin-S (ThS) fluorescence and electron microscopy (EM). It has been recently shown that tau polymerization can be monitored by measuring the increase in ThS fluorescence in the presence of tau polymers in real time (*15, 22*). This technique has shown promise, but the minimum unit of tau polymer responsible for the increase in fluorescence of ThS is still unknown. This raises the possibility that aggregates, but not necessarily tau filaments, are capable of binding to ThS and that interpretation of the resulting data could be misleading. Similarly, while electron microscopy is an invaluable tool for confirming the presence of tau filaments and elucidating their structure, it is insufficient for mechanistic analysis of tau polymerization in which numerous variables must be tested. This is due to the following facts: (1) Only a small portion of the reaction mixture can be analyzed. (2) There may be sampling errors due to differential adhesion to and/or distribution on the EM grid. (3) Grid preparation, viewing, capturing, and processing of images is cumbersome and time-consuming. (4) Difficulties in accurately quantifying the mass of filaments within an image are often experienced after long incubation periods since the filaments begin to clump together (*28*). These points have led many researchers to use EM as a qualitative tool only (*14, 18, 24, 25*). The laser light scattering (LLS) assay described herein avoids many of the pitfalls associated with ThS binding and EM.

Table 1: Summary of Polymerization Effects of the FTDP-17 Mutations

protein	i_s at steady state	apparent $t_{1/2}$ (min)	protein	i_s at steady state	apparent $t_{1/2}$ (min)
P301L	269	18	G272V	121	31
R406W	281	57	wild type (HT40)	127	64
V337M	216	46			

Light Scattering of Large Particles. The theoretical aspects of using light scattering for monitoring the size of rodlike polymers in solution have been well described elsewhere (*32, 35*) and will be mentioned only briefly here. Particles that are very small with respect to the wavelength of light ($L/\lambda < \sim 1/50$ or, in our case, $L < \sim 10$ nm, where L is the length of the particle) scatter uniformly in all directions with intensities proportional to their concentration and molecular weight, i.e., total mass (Rayleigh scattering). However, as the particle dimensions increase to become significant with respect to the wavelength of incident light, the light scattering will deviate from the ideal Rayleigh scattering in a manner dependent on the radius of gyration of the particle. In other words, for rodlike particles such as tau polymers, the total intensity of scattered light at different angles with respect to the path of the incident light can be affected by the length of the rods. However, it has been shown that when the length of rodlike particles exceeds the Berne limit (L/λ of 3.5) (*36*), the scattering intensity of a solution at any given angle is a direct measure of the mass of material polymerized (*29*).

Effects of Tau Filament Lengths on Laser Light Scattering (LLS). Since length distributions obtained by electron microscopic analysis show that the filaments formed in these experiments have not reached the Berne limit but are, on average, larger than those particles that would exhibit ideal

Rayleigh scattering, it is possible that the length of the particles could introduce an angular dependence. In other words, decreases in light scattering at 90° could, in theory, arise from the preferential forward scattering of increasingly long filaments. $P(\Theta)$ is a term which has been used to describe this deviation from ideal scattering by large particles and can be calculated from the following equation:

$$1/P(\Theta) = 1 + \frac{16\pi^2}{3\lambda^2}\langle R_G{}^2\rangle \sin^2\left(\frac{\Theta}{2}\right) \quad (3)$$

Here λ is the wavelength of light, Θ is the angle between the incident light and the observer, and R_G is the radius of gyration of the filament population (which, for long thin rods, can be approximated by $R_G = L/\sqrt{12}$) (*32*). However, for heterogeneous mixtures of differently sized particles, it is common to replace R_G with a mass average (or *z*-average) radius of gyration which is calculated by (*35*)

$$\langle R_G{}^2\rangle_z = \frac{\sum N_i L_i{}^2 (R_G{}^2)_i}{\sum N_i L_i{}^2} \quad (4)$$

where N_i is the number of filaments with a length of L_i. When the data in this report are compared to the theoretical values that are calculated from the equations above, some apparent contradictions arise. The predicted value for the average length of filaments calculated from eq 3 that have an $i_s(90°)$ of 150 and $P(40°)/P(140°)$ ratio of 1.5 is 113 nm. This is longer than the average filament length of 81 nm which was measured by electron microscopy. Conversely, the $P(40°)/P(140°)$ ratio calculated using eqs 3 and 4 and the same length distributions predicts a much larger angular dependence (3.3) than is measured (1.5). We suggest that the most likely cause for this discrepancy may be that tau filaments do not behave as rigid rods (which is a requirement for calculating R_G in eq 4). In fact, the electron micrographs show that the tau filaments are curved, suggesting a flexible structure. Therefore, as the filaments reach a certain length (perhaps greater than 100 nm), different regions of a single filament could begin to behave as spatially independent scattering units. This could conceivably result in measurements that are dependent on the length of the scattering units rather than on the filament lengths. As a result, the angular dependence of light scattering would not appreciably deviate from some maximum value, even as the filaments became very long with respect to the incident light. Our data suggest that this limit is approached even at low i_s values. The small rise in angular dependence which is observed as i_s increases is likely due to a larger percentage of the filaments reaching this limiting length.

Therefore, our data support the idea that angular dependence was insignificant in our measurements since (1) the amount of light scattering increased in a linear fashion with respect to the concentration of tau protein, (2) the angular dependence was essentially independent of the degree of polymerization, (3) the predicted value for the critical concentration of tau polymerization was similar to the value of 0.5 μM that was obtained by a method independent of particle size (ThS binding (*22*)), and (4) the agreement between the quantitation of tau polymer formation determined by LLS and electron microscopy suggest that the values obtained by LLS, like those from quantitative EM, are proportional to the polymer mass at all time points tested. Hence, the scattering detected at 90° reflects an accurate estimate of the mass of tau filaments present in the solution.

Effects of FTDP-17 Mutations on Tau Polymerization. Right angle LLS provides a physical measurement of tau polymer formation and thus allowed us to analyze the relative rate and extent of polymerization of some of the different mutant forms of the protein that are known to cause FTDP-17 (*33*). All four of the mutations tested had an effect on tau polymerization to varying degrees. The rank order of total steady state mass of polymer was P301L = R406W > V337M > G272V = wild type. Thus, three of the four mutants had a significant effect on the amount of polymer mass formed in the presence of AA. Another variable to be considered in these reactions is the apparent initial rate of polymer formation. At early time points in the polymerization, the P301L mutant appeared to have a much faster initial rate of polymerization than the other mutant forms and the wild-type tau protein. The remaining forms of tau appeared to have very similar initial rates, but they differed in the amount of time it took for the reactions to reach half-maximum amounts of polymer mass ($t_{1/2}$). G272V had an approximate $t_{1/2}$ of ~30 min, whereas R406W and V337M had approximate $t_{1/2}$ values of 45−60 min. All three of these mutant forms reached half-maximum polymer values faster than wild-type tau protein, which took longer than 60 min to attain this half-maximal value.

These results show that specific mutations in the tau molecule can cause an alteration in its assembly properties. Not only can the extent of polymerization be affected but also the rate at which the protein polymerizes. Hence, the tau mutations can affect not only the amount of tau polymers that could conceivably form within a neuron or glial cell but also the ease with which they can form. These differences in polymerization characteristics suggest that, in addition to

Table 2: Comparison of the Effects of FTDP-17 Mutations on the Polymerization of Full Length Tau Protein Performed under Different Assembly Conditions[a]

	rank order of total polymerized mass																	
A			P301L	=	P301S	>	G272V	>	WT	=	R406W	=	V337M	=	ΔK280	=	S305N	
B					P301L	>	V337M	>	WT	>	R406W							
C					R406W	>	P301L	>	WT	=	V337M							
D					P301L	>	V337M	>	WT	>	R406W							
E			P301L	=	V337M	>	R406W	>	WT									
F	P301L	=	R406W	>	V337M	>	G272V	=	WT									

[a] Key: (A) 3.0 mg/mL tau, 100−400 μg/mL heparin, 48 h at 37 °C (*17*). (B) 0.1 mg/mL tau, 10 μg/mL heparin, 48 h at 37 °C (*25*). (C) 0.1 mg/mL tau, 10 μg/mL heparin, 96 h at 37 °C (*25*). (D) 0.2 mg/mL tau, 80 μM arachidonic acid, 48 h at 37 °C (*25*). (E) 0.2 mg/mL tau, 80 μM arachidonic acid, 96 h at 37 °C (*25*). (F) 0.2 mg/mL tau, 75 μM arachidonic acid, 7 h at room temperature (this study).

other functional alterations of the protein such as effects on microtubule binding and the promotion of microtubule assembly (*37*), the tau mutations can lead directly to increased amounts of protein polymerization. Thus, the formation of tau polymers may drastically impair intracellular transport events as do neurofilament aggregations in mouse models of lower motor neuron disease (*38*).

Comparison with Previous Work. Other laboratories have documented an effect of FTDP-17 mutations on the polymerization of tau. Although many of these mutations reportedly increased tau polymerization, there remains disagreement as to which affect this process most (summarized in Table 2). These differences most likely arise from the disparity of techniques used to induce and subsequently quantify tau polymerization. The difference in the inducer molecule which is used (either heparin or arachidonic acid) is very likely one source of variability. Another difference is the concentration of protein employed for the assays (2−60 μM). Finally, different methods were used to quantify filament mass: qualitative scoring using EM (*17*); a mixture of quantitative and qualitative EM (*25*); LLS (this report). Although these differences make a direct comparison difficult, P301L stands out as one mutant that all three studies agree upon as having a significant positive effect on tau polymerization (Table 2). Overall, our results agree most closely with the AA induction results of Nacharaju et al. (1999) obtained after 4 days of induction, where they describe P301L, V337M, and R406W as polymerizing better than wild type.

Conclusion. Our data have shown LLS to be an efficient physical measurement of the polymerized mass of tau polymers. It is our contention that LLS is an excellent candidate for a common method to monitor the polymerization of tau, regardless of the concentration of protein or the nature of the inducer used. Such a common method would greatly enhance future studies in the field of tau polymerization and allow more meaningful comparisons of results obtained in different laboratories.

ACKNOWLEDGMENT

We are deeply grateful for the efforts of Dr. Guenter Albrecht-Buehler in designing and building the right angle laser light scattering apparatus and for the use of his software to operate the camera. We thank Dr. Robley C. Williams, Jr., for his helpful suggestions during the preparation of the manuscript. We also thank E. Cartman for advice and encouragement.

REFERENCES

1. Delacourte, A., and Buee, L. (1997) *Int. Rev. Cytol. 171*, 167−224.
2. Spillantini, M. G., and Goedert, M. (1998) *Trends Neurosci. 21*, 428−33.
3. Arriagada, P. V., Growdon, J. H., Hedley-Whyte, E. T., and Hyman, B. T. (1992) *Neurology 42*, 631−9.
4. Braak, H., and Braak, E. (1991) *Acta Neuropathol. 82*, 239−59.
5. Spillantini, M. G., Crowther, R. A., Kamphorst, W., Heutink, P., and van Swieten, J. C. (1998) *Am. J. Pathol. 153*, 1359−63.
6. Spillantini, M. G., Murrell, J. R., Goedert, M., Farlow, M. R., Klug, A., and Ghetti, B. (1998) *Proc. Natl. Acad. Sci. U.S.A. 95*, 7737−41.
7. Poorkaj, P., Bird, T. D., Wijsman, E., Nemens, E., Garruto, R. M., Anderson, L., Andreadis, A., Wiederholt, W. C., Raskind, M., and Schellenberg, G. D. (1998) *Ann. Neurol. 43*, 815−25.
8. Nasreddine, Z. S., Loginov, M., Clark, L. N., Lamarche, J., Miller, B. L., Lamontagne, A., Zhukareva, V., Lee, V. M., Wilhelmsen, K. C., and Geschwind, D. H. (1999) *Ann. Neurol. 45*, 704−15.
9. Hutton, M., Lendon, C. L., Rizzu, P., Baker, M., Froelich, S., Houlden, H., Pickering-Brown, S., Chakraverty, S., Isaacs, A., Grover, A., Hackett, J., Adamson, J., Lincoln, S., Dickson, D., Davies, P., Petersen, R. C., Stevens, M., de Graaff, E., Wauters, E., van Baren, J., Hillebrand, M., Joosse, M., Kwon, J. M., Nowotny, P., Heutink, P., et al. (1998) *Nature 393*, 702−5.
10. Dumanchin, C., Camuzat, A., Campion, D., Verpillat, P., Hannequin, D., Dubois, B., Saugier-Veber, P., Martin, C., Penet, C., Charbonnier, F., Agid, Y., Frebourg, T., and Brice, A. (1998) *Hum. Mol. Genet. 7*, 1825−9.
11. D'Souza, I., Poorkaj, P., Hong, M., Nochlin, D., Lee, V. M., Bird, T. D., and Schellenberg, G. D. (1999) *Proc. Natl. Acad. Sci. U.S.A. 96*, 5598−603.
12. Clark, L. N., Poorkaj, P., Wszolek, Z., Geschwind, D. H., Nasreddine, Z. S., Miller, B., Li, D., Payami, H., Awert, F., Markopoulou, K., Andreadis, A., D'Souza, I., Lee, V. M., Reed, L., Trojanowski, J. Q., Zhukareva, V., Bird, T., Schellenberg, G., and Wilhelmsen, K. C. (1998) *Proc. Natl. Acad. Sci. U.S.A. 95*, 13103−7.
13. Foster, N. L., Wilhelmsen, K., Sima, A. A., Jones, M. Z., D'Amato, C. J., and Gilman, S. (1997) *Ann. Neurol. 41*, 706−15.
14. Goedert, M., Jakes, R., Spillantini, M. G., Hasegawa, M., Smith, M. J., and Crowther, R. A. (1996) *Nature 383*, 550−3.
15. Friedhoff, P., Schneider, A., Mandelkow, E. M., and Mandelkow, E. (1998) *Biochemistry 37*, 10223−30.
16. Arrasate, M., Perez, M., Armas-Portela, R., and Avila, J. (1999) *FEBS Lett. 446*, 199−202.
17. Goedert, M., Jakes, R., and Crowther, R. A. (1999) *FEBS Lett. 450*, 306−11.
18. Hasegawa, M., Crowther, R. A., Jakes, R., and Goedert, M. (1997). *J. Biol. Chem. 272*, 33118−24.
19. Perez, M., Valpuesta, J. M., Medina, M., Montejo de Garcini, E., and Avila, J. (1996) *J. Neurochem. 67*, 1183−90.
20. Kampers, T., Friedhoff, P., Biernat, J., Mandelkow, E. M., and Mandelkow, E. (1996) *FEBS Lett. 399*, 344−9.
21. Wilson, D. M., and Binder, L. I. (1997) *Am. J. Pathol. 150*, 2181−95.
22. King, M. E., Ahuja, V., Binder, L. I., and Kuret, J. (1999) *Biochemistry 38*, 14851−14859.
23. Schneider, A., Biernat, J., von Bergen, M., Mandelkow, E., and Mandelkow, E. M. (1999) *Biochemistry 38*, 3549−58.
24. Wille, H., Drewes, G., Biernat, J., Mandelkow, E. M., and Mandelkow, E. (1992) *J. Cell. Biol. 118*, 573−84.
25. Nacharaju, P., Lewis, J., Easson, C., Yen, S., Hackett, J., Hutton, M., and Yen, S. H. (1999) *FEBS Lett. 447*, 195−9.
26. Wilson, D. M., and Binder, L. I. (1995) *J. Biol. Chem. 270*, 24306−14.
27. Montejo de Garcini, E., and Avila, J. (1987) *J. Biochem. (Tokyo) 102*, 1415−21.
28. King, M. E., Gamblin, T. C., Kuret, J., and Binder, L. I. (2000) *J. Neurochem. 74*, 1749−1757.
29. Gaskin, F., Cantor, C. R., and Shelanski, M. L. (1974) *J. Mol. Biol. 89*, 737−55.
30. Mukherjee, A., and Lutkenhaus, J. (1999) *J. Bacteriol. 181*, 823−32.
31. Carmel, G., Leichus, B., Cheng, X., Patterson, S. D., Mirza, U., Chait, B. T., and Kuret, J. (1994) *J. Biol. Chem. 269*, 7304−7309.
32. Van Holde, K. E. (1971) *Physical Biochemistry*, Prentice-Hall, Englewood Cliffs, NJ.
33. Goedert, M., Crowther, R. A., and Spillantini, M. G. (1998) *Neuron 21*, 955−8.

34. Hall, G. F., Yao, J., and Lee, G. (1997) *Proc. Natl. Acad. Sci. U.S.A. 94*, 4733−8.
35. Tanford, C. (1961) *Physical Chemistry of Macromolecules*, John Wiley & Sons, Inc., New York.
36. Berne, B. J. (1974) *J. Mol. Biol. 89*, 755−8.
37. Hong, M., Zhukareva, V., Vogelsberg-Ragaglia, V., Wszolek, Z., Reed, L., Miller, B. I., Geschwind, D. H., Bird, T. D., McKeel, D., Goate, A., Morris, J. C., Wilhelmsen, K. C., Schellenberg, G. D., Trojanowski, J. Q., and Lee, V. M. Y. (1998) *Science 282*, 1914−7.
38. Xu, Z., Cork, L. C., Griffin, J. W., and Cleveland, D. W. (1993) *Cell 73*, 23−33.

BI000201F